Materials Research Proceedings 69 (2026) 564-570 https://doi.org/10.21741/9781644904251-101

GPU-Accelerated CABARET Simulations of Distributed Propulsion for UAM

Hussain A. ABID[1,2,a], Igor SOLNTSEV[2], Andrea RAPISARDA[3], Hassan A. ABID[4], Sergey A. KARABASOV[1,2], E. DE PAOLA[5], Luana Georgiana STOICA[5], Giorgia CAPOBIANCHI[5], Alessandro DI MARCO[5], R. CAMUSSI[5]

[1]School of Engineering and Materials Science, Queen Mary University of London, Mile End Road, London, E1 4NS, UK

[2]GPU-prime Ltd, Cambridge, UK

[3]Department of Civil, Environmental and Mechanical Engineering, University of Trento, Via Mesiano, 77, 38123 Trento, IT

[4]Department of Aerospace Engineering, King Fahd University of Petroleum and Minerals (KFUPM), Dhahran, Saudi Arabia

[5]Department of Engineering, Roma Tre University, Via Vito Volterra, 62, Rome, 00146, RM, Italy

[a]h.abid@qmul.ac.uk

Keywords: Distributed Propulsion, Urban Air Mobility, CABARET Method, Large Eddy Simulation, Rotating Meshes, Aeroacoustics, Trailing-Edge Serrations

Abstract. Urban Air Mobility (UAM) vehicles rely on distributed propulsion (DP) to achieve efficiency, control authority, and compact integration with lifting surfaces. The close spacing of multiple rotors, however, intensifies installation effects that elevate tonal and broadband noise. This work presents a high-fidelity Large Eddy Simulation (LES) study using the CABARET method on rotating meshes to quantify aeroacoustic and aerodynamic sensitivities of a three-propeller DP configuration. The campaign varies: (i) central-rotor axial position ($\Delta x = \{-0.2Db, 0, +0.2Db\}$), (ii) inter-rotor phase angle ($0°, 45°, 90°, 135°$), and(iii) blade trailing-edge geometry (baseline vs. sawtooth serrations). Band-limited overall sound pressure level (BL OASPL) is evaluated on a probe plane under the array between the 1st and 6th blade-passing frequencies. Key findings are: (a) serrations consistently reduce area-averaged and maximum BL OASPL by up to 2.4 dB, most notably around 90◦ phase; (b) moving the central rotor closer to the wing increases thrust coefficient by ≈ 7.8%, indicating a beneficial rotor–wing interaction akin to ground effect; (c) the aerodynamic penalty of serrations is modest and attributable to effective area loss near the tip. Flow visualizations show serrations disrupt spanwise coherence and trailing-edge vortex organization, explaining the observed acoustic benefits. The results highlight the importance of joint optimization of geometry and phasing to deliver quieter, efficient DP systems for UAM.

1. Introduction

UAM concepts increasingly adopt DP to distribute thrust and to leverage propeller–wing interaction for lift augmentation and control [1, 2, 3, 4]. Compact layouts, however, amplify noise through periodic wake–airframe interactions (tonal peaks at blade-passing harmonics) and broadband mechanisms associated with boundary-layer and wake turbulence [5, 6, 7, 8]. Prior work shows strong sensitivity of noise directivity and level to rotor placement and phasing relative to wings [9, 10, 11]. Passive serrated trailing edges, inspired by owl feathers, can reduce scattering efficiency and spanwise coherence [12, 13, 14, 15, 16, 17, 18]. Here we assess, within one

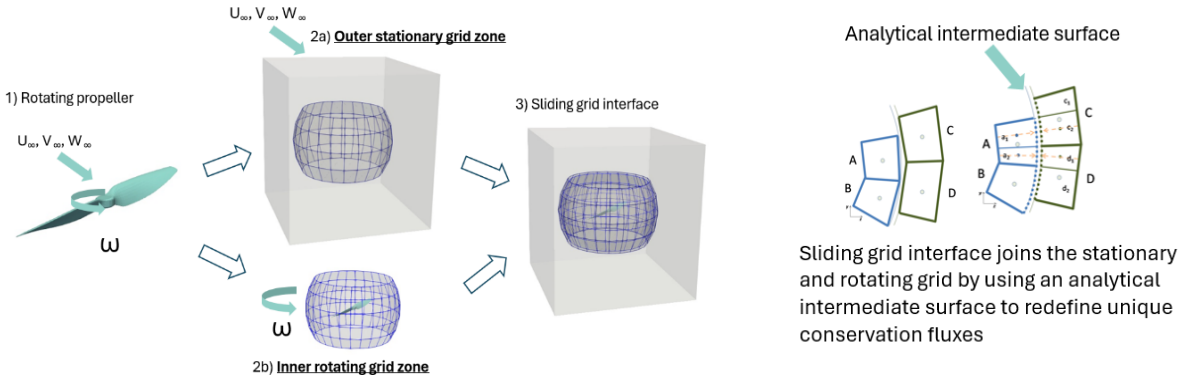
Content from this work may be used under the terms of the Creative Commons Attribution 3.0 license. Any further distribution of this work must maintain attribution to the author(s) and the title of the work, journal citation and DOI. Published under license by Materials Research Forum LLC.

Materials Research Proceedings 69 (2026) 564-570 https://doi.org/10.21741/9781644904251-101

consistent LES framework, how axial position, phase, and serrations jointly govern the aeroacoustic signature of a representative three-rotor DP system based on TU Delft experiments [19].

2. Numerical Methodology

We employ a GPU-accelerated CABARET LES on rotating meshes [19, 20, 21, 22, 23]. Sliding interfaces conserve fluxes via a super-mesh projection and compact sub-cell reconstructions, preserving the dispersion and dissipation properties of the base scheme while avoiding re-meshing.



(a) Rotating and stationary zones with sliding interface. (b) *Analytical interface for conservative fluxing.*

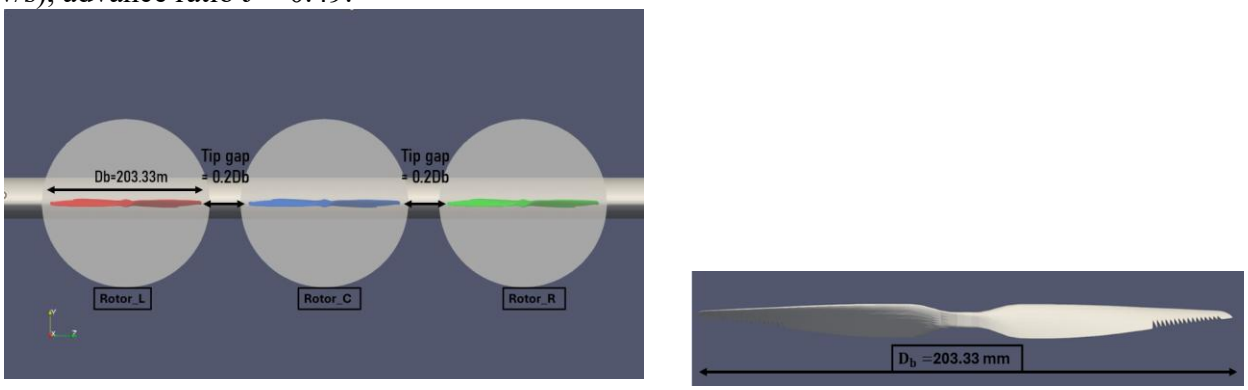
Figure 1: CABARET LES rotating-mesh formulation.

2.1 LES CABARET Solver

An improved-dispersion variant and asynchronous time-stepping enhance accuracy and efficiency. Wall modelling adopts Reichardt's law; the solver is MPI parallel and GPU-resident to minimize turnaround time. Prior validations include a single propeller in boundary-layer ingestion configurations [24].

2.2 Test Cases and Parametric Study

Three identical two-bladed Mejzlik propellers of diameter $D_b = 203.33\,mm$ are aligned span-wise and located 220 mm upstream of a wing leading edge; the central rotor (Rotor$_C$) translates axially by $\pm 0.2D_b$, while lateral rotors remain fixed. The phase of Rotor$_C$ relative to the others is set to 0◦, 45◦, 90◦, 135◦. Serrations (sawtooth, 16 wedges from r = 63.5–88.5 mm, depth 2.32 mm, spacing ≈ 1.55 mm) follow guidelines in [14]. Operating point: U∞ = 30 m/s, n = 5730 RPM (95.5 rev/s), advance ratio J = 0.49.



(a) Three-rotor configuration upstream of the wing. *(b) Serrated trailing-edge geometry.*

Figure 2: Configuration and serration concept used in the study.

Materials Research Proceedings 69 (2026) 564-570 https://doi.org/10.21741/9781644904251-101

2.3 Numerical grid
ANSYS ICEM generates hexahedral meshes with rotating zones around each rotor and a stationary outer domain. The domain extends $5D_b$ upstream and $10D_b$ downstream of the wing. Grids contain ~ 5.1M cells (serrated) and ~ 4.9M (baseline), refined near blades, wakes, and the wing.

2.4 Noise footprint of the DEP system
Pressure probes populate a plane at z = $-1D_b$ beneath the array to evaluate BL OASPL between the 1st and 6th BPFs. We report (i) area-averaged BL OASPL and (ii) maximum BL OASPL across all probes.

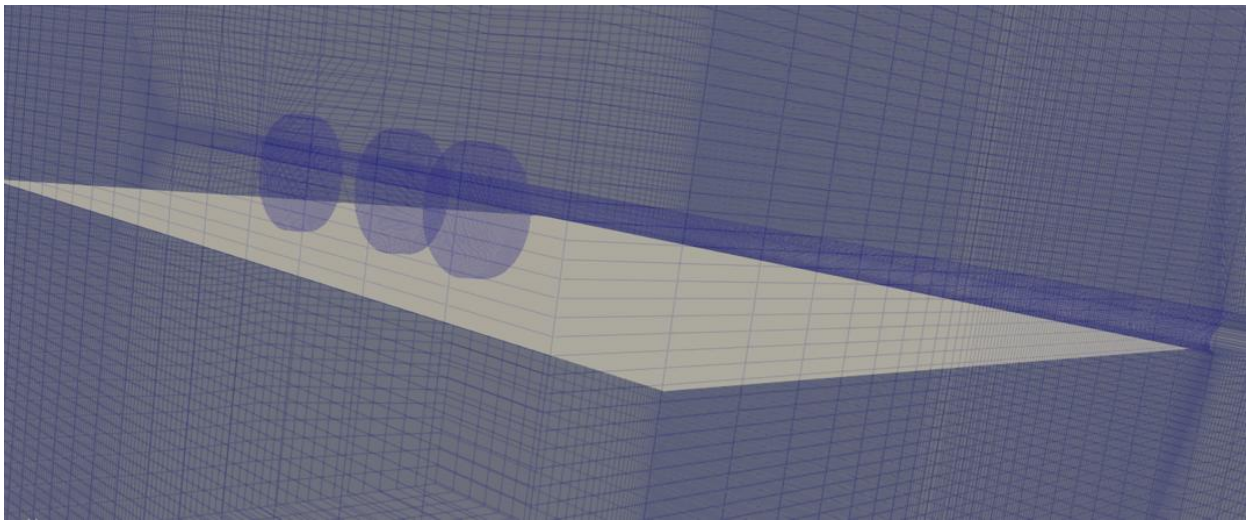


Figure 3: Probe plane used for BL OASPL evaluation beneath the rotors.

3. Results and Discussion

3.1 Aerodynamic Results
Rotor performance is characterized by thrust and torque coefficients:

$$C_T = \frac{T}{\rho n^2 D^4}, \qquad C_Q = \frac{T}{\rho n^2 D^5} \tag{1}$$

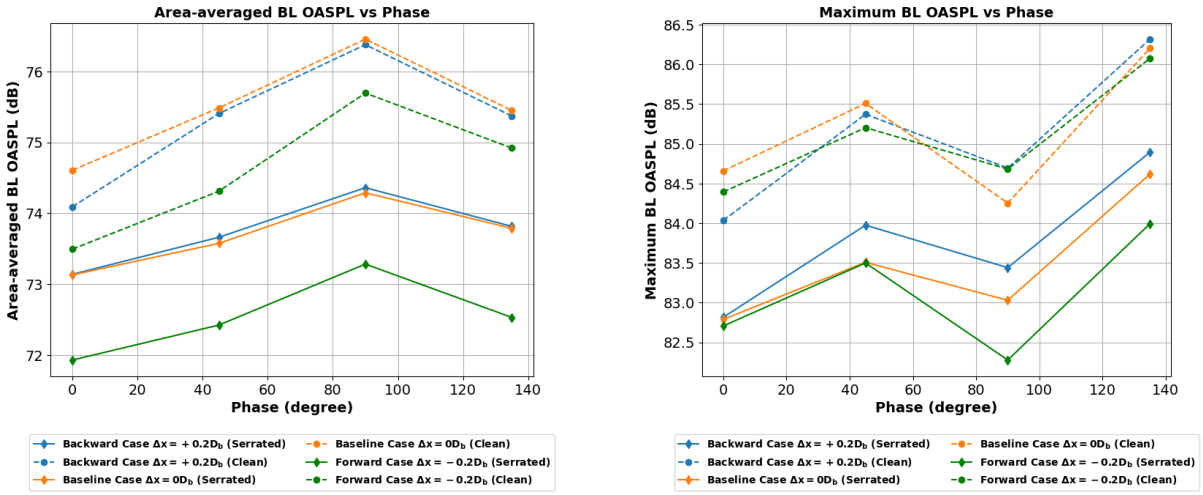
At fixed RPM and J, axial translation of Rotor$_C$ modulates rotor–wing interaction. Bringing Rotor$_C$ closer to the wing increases C_T by ≈ 7.8% relative to the baseline, consistent with an effective ground-effect mechanism that boosts induced velocities and pressure recovery below the disk. Phase primarily affects unsteady interference rather than mean thrust; thus, C_T is comparatively insensitive to phase. Serrations slightly reduce C_T (and C_Q) due to effective area loss near the tip, matching the expected aerodynamic trade-off.

3.2 Flow Field
Baseline blades shed coherent trailing-edge and tip structures whose interaction with the wing drives unsteady loading. Serrations fragment large coherent vortices into weaker, shorter-coherence structures, reducing spanwise correlation of surface pressure fluctuations. The resulting wake has diminished organized content at BPF harmonics, a precondition for lower tonal and mid-to-high-frequency broadband emissions.

3.3 Acoustic Pressure Fluctuations
Figure 4 summarizes BL OASPL trends versus phase for axial positions. Serrations reduce both area-averaged and maximum BL OASPL across all cases, with the largest benefit near 90°. Forward axial offset ($\Delta x = -0.2D_b$) generally yields the lowest BL OASPL; the backward case shows smaller gains, indicating geometry-dependent engagement of the serration mechanism with

Materials Research Proceedings 69 (2026) 564-570 https://doi.org/10.21741/9781644904251-101

installation effects. The peak reduction of ≈ 2.4 dB aligns with small-scale experimental ranges in the literature for sawtooth treatments [25, 26, 27] and with analytical predictions of coherence suppression [28, 29, 30, 31].



(a) Area-averaged BL OASPL vs. phase. *(b) Maximum BL OASPL vs. phase.*

Figure 4: Noise metrics for baseline and serrated blades across axial positions.

4. Conclusion

A GPU-accelerated CABARET LES framework was applied to a three-rotor DP system typical of UAM installations. We varied axial position, inter-rotor phase, and trailing-edge geometry to isolate drivers of aeroacoustic performance. Serrated trailing edges achieved up to 2.4 dB reductions in both maximum and area-averaged BL OASPL, with strongest gains near 90◦ phase. Moving the central rotor closer to the wing increased C_T by ≈ 7.8%, evidencing beneficial rotor–wing coupling; serrations incurred a modest aerodynamic penalty.

Flow analyses support a mechanism of reduced spanwise coherence and disrupted vortex organization. The combined results indicate that optimizing rotor placement, phasing, and serration geometry is essential to simultaneously mitigate noise and retain efficiency in DP architectures. Future work will extend to alternative serration metrics, flap-equipped wings, and advance-ratio sweeps to map robustness across flight phases.

5. Additional work to be reported on full paper

Noise directivity results of the above considered three propeller-wing configurations will be compared with the available experimental results of the 3D wing-flap and three electric motor-driven propellers in a similar ‘puller’ propeller setup. The latter setup corresponds to the recent H2020 CS2 European project VENUS, which investigated methodologies and tools to enable a concurrent design approach for both the aerodynamics and aeroacoustics of aircraft focusing on DEP. The details about the work are presented in DePaola et al. [32] The experimental tests comprise both measurements of acoustics and aerodynamics. A particular finding of the VENUS campaign was that the largest effect on DP noise was due to the propeller wake interaction with the deployed wing flap. Therefore, the best noise reduction was found for the propellers positioned closest to the wing.

In comparison with the VENUS configuration, the ENODISE setup does not include a deployed flap, and the best reduction there appears to correspond to the largest distance between the propellers in the forward staggered configuration. Nevertheless, regardless of the specific propeller/wing geometry details it is interesting to compare the acoustic directivity of the overall noise reduction achieved by changing the propeller installation with respect to the wing in the

ENODISE and VENUS DP configurations. This comparison will be performed for similar offset phase angles of the central propeller, with and without applying the noise reduction technique (trailing edge serrations) in case of the ENODISE propellers. Details will be reported in the full paper along with the LES grid sensitivity study.

In addition, aerodynamic performance of different DEP configurations corresponding to the ENODISE setup will be analyzed as well as the far-field noise will be computed based on the Ffwocs Williams-Hawkings's method. This will allow us to assess the trade-off between the aerodynamic and the aeroacoustic performance for the considered ENODISE DEP configuration, like the experimental investigation in the VENUS project.

References

[1] Nicholas K Borer, Michael D Patterson, Jeffrey K Viken, Mark D Moore, Joe Ben Bevirt, Alex M Stoll, and Andrew R Gibson. Design and performance of the NASA sector distributed electric propulsion flight demonstrator. In 16th AIAA aviation technology, integration, and operations conference, page 3920, 2016. https://doi.org/10.2514/6.2016-3920

[2] Jean Hermetz, Michael Ridel, and Carsten Doll. Distributed electric propulsion for small business aircraft a concept-plane for key-technologies investigations. In ICAS 2016, 2016.

[3] Reynard de Vries, Nando van Arnhem, Tomas Sinnige, Roelof Vos, and Leo L. M. Veldhuis. Aerodynamic interaction between propellers of a distributed-propulsion system in forward flight. Aerospace Science and Technology, 118:107009, 2021. https://doi.org/10.1016/j.ast.2021.107009

[4] Michael D Patterson, Joseph M Derlaga, and Nicholas K Borer. High-lift propeller system configuration selection for NASA's sector distributed electric propulsion flight demonstrator. In 16th AIAA aviation technology, integration, and operations conference, page 3922, 2016. https://doi.org/10.2514/6.2016-3922

[5] Hyun D. Kim, Aaron T. Perry, and Phillip J. Ansell. A Review of Distributed Electric Propulsion Concepts for Air Vehicle Technology.

[6] Tian Zhou and Rami Fattah. Tonal noise acoustic interaction characteristics of multi-rotor vehicles. In 23rd AIAA/CEAS Aeroacoustics Conference, page 4054, 2017. https://doi.org/10.2514/6.2017-4054

[7] J. Thauvin, Guillaume Barraud, Marc Budinger, Xavier Roboam, Dimitri Leray, and Bruno Sareni. Hybrid regional aircraft: A comparative review of new potentials enabled by electric power. In 52nd AIAA/SAE/ASEE joint propulsion conference, page 4612, 2016. https://doi.org/10.2514/6.2016-4612

[8] J. E. Barker, A. Zarri, J. Christophe, and C. F. Schram. Numerical investigation of tonal noise emissions from propeller-wing aerodynamic and acoustic interactions. In AIAA Aviation 2023 Forum, 2023. https://doi.org/10.2514/6.2023-4056

[9] Tomas Sinnige, Nando van Arnhem, Tom C. A. Stokkermans, Georg Eitelberg, and Leo L. M. Veldhuis. Wingtip-mounted propellers: Aerodynamic analysis of interaction effects and comparison with conventional layout. Journal of Aircraft, 56(1):295-312, 2019. https://doi.org/10.2514/1.C034978

[10] Andrea Zarri, Athanasios Koutsoukos, and Francesco Avallone. Aerodynamic and acoustic interaction effects of adjacent propellers in forward flight. In 29th AIAA/CEAS Aeroacoustics Conference, page 4489, 2023. https://doi.org/10.2514/6.2023-4489

[11] Z. Yang, M. Meinke, and W. Schroder. Numerical analysis of propeller-airfoil interaction in a distributed propulsion system using a hybrid les and fw-h approach. In AIAA Aviation Forum, page 3211, 2024. https://doi.org/10.2514/6.2024-3211

[12] M. S. Howe. Aerodynamic noise of a serrated trailing edge. Journal of Fluids and Structures, 5(1):33-45, 1991. https://doi.org/10.1016/0889-9746(91)80010-B

[13] M. S. Howe. Noise produced by a sawtooth trailing edge. The Journal of the Acoustical Society of America, 90(1):482-487, 1991. https://doi.org/10.1121/1.401273

[14] M. Gruber. Airfoil noise reduction by edge treatments. PhD thesis, University of Southampton, 2012.

[15] B. Lyu, M. Azarpeyvand, and S. Sinayoko. Prediction of noise from serrated trailing edges. Journal of Fluid Mechanics, 793:556-588, 2016. https://doi.org/10.1017/jfm.2016.132

[16] T. P. Chong and A. Vathylakis. On the aeroacoustic and flow structures developed on a flat plate with a serrated sawtooth trailing edge. Journal of Sound and Vibration, 354:65-90, 2015. https://doi.org/10.1016/j.jsv.2015.05.019

[17] C. Arce-Leo'n, R. Merino-Mart'ınez, D. Ragni, F. Avallone, and M. Snellen. Boundary layer characterization and acoustic measurements of flow-aligned trailing edge serrations. Experiments in Fluids, 57(182), 2016. https://doi.org/10.1007/s00348-016-2272-z

[18] T. P. Chong, P. F. Joseph, and M. Gruber. Airfoil self-noise reduction by non-flat plate type trailing edge serrations. Applied Acoustics, 74(4):607-613, 2013. https://doi.org/10.1016/j.apacoust.2012.11.003

[19] I. Solntsev, A Chintagunta, A Markesteijn, and S Karabasov. Cabaret on rotating meshes. Elsevier Applied Mathematics and Computation, 2023. https://doi.org/10.1016/j.amc.2023.127871

[20] Anton P. Markesteijn and Sergey A. Karabasov. Cabaret solutions on graphics processing units for NASA jets: Grid sensitivity and unsteady inflow condition effect. Comptes Rendos M'ecanique, 346(10):948-963, 2018. Jet noise modelling and control Modelisation et controle du bruit de jet. https://doi.org/10.1016/j.crme.2018.07.004

[21] Vasily A. Semiletov and Sergey A. Karabasov. A volume integral implementation of the Goldstein generalized acoustic analogy for unsteady flow simulations. Journal of Fluid Mechanics, 853:461-487, 2018. https://doi.org/10.1017/jfm.2018.572

[22] Georgy A. Faranosov, Vasily M. Goloviznin, Sergey A. Karabasov, Vasily G. Kondakov, Victor F. Kopiev, and Mihail A. Zaitsev. Cabaret method on unstructured hexahedral grids for jet noise computation. Computers and Fluids, 88:165-179, 2013. https://doi.org/10.1016/j.compfluid.2013.08.011

[23] V.A. Semiletov and S.A. Karabasov. Cabaret scheme for computational aero acoustics: Extension to asynchronous time stepping and 3d flow modelling. International Journal of Aeroacoustics, 13(3-4):321-336, 2014. https://doi.org/10.1260/1475-472X.13.3-4.321

[24] Hussain Ali Abid, Sergey A. Karabasov, Annabel P. Markesteijn, and Igor Solntsev. Numerical investigation of propeller boundary layer ingestion noise using cabaret on rotating meshes. In 30th AIAA/CEAS Aeroacoustics Conference, Rome, Italy, June 2024.

[25] Weicheng Ning, Shaohong Jia, Hongyu Wang, Zhe Chen, and Bing Yang. An experimental study on small UAV propellers with serrated trailing edges. AIAA Journal, 2017. UAV-scale tests showed 0.9-1.6dB noise reduction. https://doi.org/10.2514/6.2017-3813

[26] Weicheng Xue et al. An experimental study of noise reduction in wind turbine airfoils with serrated trailing edges. arXiv preprint arXiv:2307.12188, 2023. Sawtooth serrations reduced noise by 2.7-3.0dB with thrust preservation.

[27] A. Rapisarda, L. Sangiuliano, L. D'Alessandro, and N. M. Pugno, Bio-inspired rotor designs: enhancing thrust, energy efficiency, and noise reduction,' Bioinspiration & Biomimetics, Nov. 28, 2025. https://doi.org/10.1088/1748-3190/adf6f8

[28] B. Lyu, Mahdi Azarpeyvand, and Samuel Sinayoko. Prediction of noise from serrated trailing-edges. Journal of Fluid Mechanics, 793:1-29, 2016. Analytical model predicts noise reduction up to 10dB at 90°. https://doi.org/10.1017/jfm.2016.132

[29] D. J. Moreau and C. J. Doolan. Noise-reduction mechanism of a flat-plate serrated trailing edge. AIAA Journal, 51(10):2513-2524, 2013. https://doi.org/10.2514/1.J052436

[30] Samuel Sinayoko, B. Lyu, and M. Azarpeyvand. Prediction of noise from serrated trailing-edges (AIAA 2015). AIAA/CEAS Aeroacoustics Conference, 2015. Provided advanced analytical model validating serration performance.

[31] F. Avallone, W. C. P. Van der Velden, D. Ragni, and D. Casalino, Noise reduction mechanisms of sawtooth and combed-sawtooth trailing-edge serrations. Journal of Fluid Mechanics, 848:560-591, 2018. Confirmed geometry- and phase-dependent trends. https://doi.org/10.1017/jfm.2018.377

[32] Emanuele De Paola, Andrea Di Marco, Laurentiu G. Stoica, Luca Falcini, and Roberto Camussi. Experimental investigation on a side-by-side twin rotor system in pusher configuration. In INTER-NOISE and NOISE-CON Congress and Conference Proceedings, volume 265, pages 5862-5872, 2023. https://doi.org/10.3397/IN_2022_0870